IUCrData

ISSN 2414-3146

4-Amino-3,5-dichloropyridine

Thankappan Ramalakshmi Anantheeswary,[a] Sundaramoorthy Gomathi,[a]* Ramu Shyamaladevi,[a] Samson Jegan Jennifer[b] and Ibrahim Abdul Razak[c]

[a]Department of Chemistry, Periyar Maniammai Institute of Science & Technology, Thanjavur, Tamilnadu-613403, India, [b]Department of Chemistry, Bishop Heber College, Tiruchirappalli, Tamilnadu-620017, India, and [c]X-ray Crystallography Unit, School of Physics, University Sains Malaysia, 11800, USM, Penang, Malaysia. *Correspondence e-mail: gomathichemist@pmu.edu

Received 25 September 2024
Accepted 18 November 2024

Edited by R. J. Butcher, Howard University, USA

Keywords: 4-amino-3,5-dichloropyridine; crystal structure; offset π–π stacking; halogen–π interaction. Hirshfeld surface analysis.

CCDC reference: 2403603

Structural data: full structural data are available from iucrdata.iucr.org

The title compound, $C_5H_4Cl_2N_2$, crystallizes with one molecule in the asymmetric unit. In the crystal, the molecular entities are assembled through strong N—H···N hydrogen bonding, forming supramolecular chains extending along the *b*-axis direction. These chains are interconnected by offset π–π stacking interactions and consolidated by halogen–π interactions. The molecular interactions were quantified by Hirshfeld surface analysis, showing the significant contributions of Cl···H/H···Cl (40.1%), H···H (15.7%) and N···H / H···N (13.1%) interactions. Energy framework analysis using the CE-B3LYP/6–31 G(d,p) basis set revealed that Coulombic interactions make a considerable contribution to the total energy and crystal packing.

3D view

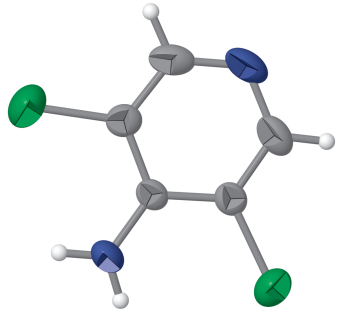

Chemical scheme

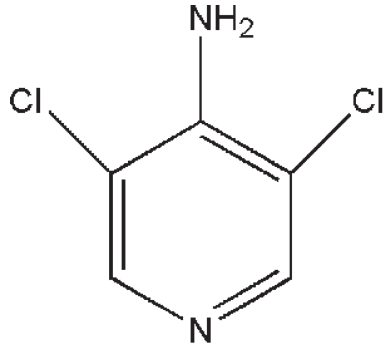

Structure description

4-Amino-3,5-dichloropyridine (ADCP) is of interest in organic synthesis and medicinal chemistry due to its versatile reactivity and potential properties including antimicrobial (Singaram *et al.*, 2016) and anti-cancer (Onnis *et al.*, 2009) activity. Its derivatives are employed in the development of drugs targeting various biological inflammatory diseases (Boland *et al.*, 2014), bacterial infections (Chung *et al.*, 1999) and hyperthyroidism. Structural studies of chloro and dichloropyridine derivatives, namely 2-amino-3-chloropyridine (Hu *et al.*, 2011), 2-amino-5-chloropyridine-fumaric acid (Hemamalini & Fun, 2010), 2-amino-3,5-dichloropyridinium chloride monohydrate (Anagnostis & Turnbull, 1998) and 4-amino-3,5-dichloropyridinium 3-hydroxypicolinate monohydrate (Ashokan *et al.*, 2023) have been reported in the literature. The crystal structure of ADCP will be helpful in identifying the structural and supramolecular patterns that play a significant role in its functional properties.

The asymmetric unit of ADCP (Fig. 1) consists of one molecule. The C1—N1—C5 bond angle is 116.4 (5)°, indicating that the ring nitrogen atom of ADCP is sp^2 hybridized

OPEN ACCESS
Published under a CC BY 4.0 licence

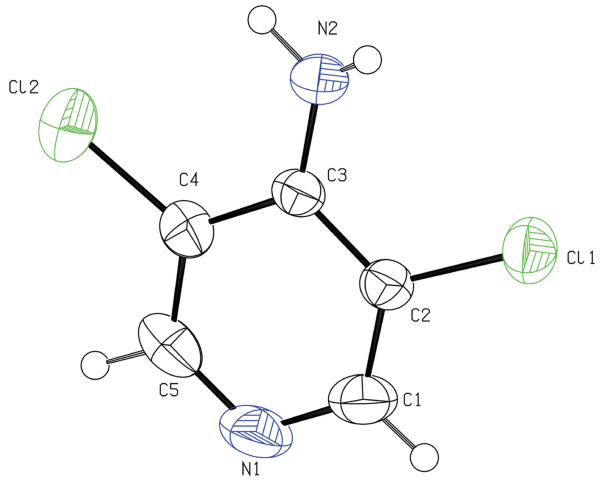

Figure 1
ORTEP view of ADCP with displacement ellipsoids drawn at the 50% probability level.

(Newell *et al.*, 2022). The deviation from the ideal angle of 120° is due to the strain exerted by the presence of a lone pair on the nitrogen atom and contributes to the weak basicity of ADCP. In the crystal, the molecular entities are assembled through N—H···N hydrogen bonding between the amino N2 atom and ring N1 atom of a symmetry-related molecule (Table 1), forming supramolecular chains along the *b*-axis direction. Neighbouring chains are interlinked by offset aromatic π–π stacking interactions (Malenov & Zarić, 2023) between the pyridine π clouds [$Cg1\cdots Cg1(x, y, 1 + z)$ = 3.8638 (19) Å, perpendicular distance = 3.4954 (12) Å and slip angle = 25.2° where $Cg1$ is the centroid of the N1/C1–C5 ring; symmetry code: $x, y, 1 + z$], as shown in Fig. 2. The cohesion of the crystal structure is enhanced by the presence of halogen–π interactions (Rahman *et al.*, 2003) with a Cl···π distance of = 3.9375 (17) Å.

Hirshfeld surface (HS) (McKinnon *et al.*, 2007; Spackman & Jayatilaka, 2009) analysis was used to visualize and quantify the intermolecular interactions in the crystal. The isovalue of w(r)= 1/2, mapped over d_{norm} on the HS to the inside (d_i) and exterior (d_e) atoms between the arbitrary units (−0.46 to 1.21) specifies the HS of ADCP. The intensity of the hydrogen-bonded contacts in the HS of ADCP are represented as red, blue, and white in Fig. 3. The strongest interactions are indicated by red, weaker interactions are represented by white, and interactions larger than the total of the van der Waals radii of neighbouring atoms are indicated by blue. The acceptor regions of hydrogen bonds are highlighted in red on the d_{norm}

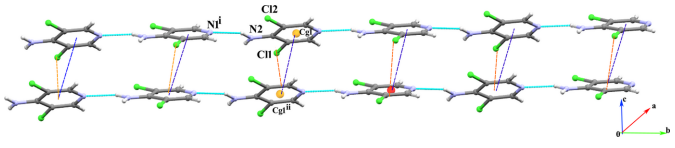

Figure 2
Supramolecular chains formed through N—H···N hydrogen bonds and interlinked *via* offset aromatic π–π stacking and halogen–π interactions. [Symmetry codes: (i) $\frac{1}{2} - x, \frac{1}{2} + y, \frac{1}{2} + z$; (ii) $x, y, 1 + z$.]

Table 1
Hydrogen-bond geometry (Å, °).

D—H···A	D—H	H···A	D···A	D—H···A
N2—H1A···Cl1^{i}	0.84 (4)	2.81 (4)	3.625 (3)	164 (3)
N2—H2A···N1^{ii}	0.85 (2)	2.16 (3)	2.931 (3)	149 (3)

Symmetry codes: (i) $-x + 1, -y + 1, z + \frac{1}{2}$; (ii) $-x + \frac{1}{2}, y + \frac{1}{2}, z + \frac{1}{2}$.

surface. The HS plotted over d_{norm} shows the atoms within 3.8 Å of the HS, showing the strong N—H···N intermolecular hydrogen-bonding interactions linking 4-amino N2 and ring N1 atoms of adjacent ADCP molecules.

The presence of π–π stacking interactions is indicated and confirmed by the contiguous red and blue triangular regions around the pyridine rings on the HS mapped over the shape index (see Fig. 4). The stacking interaction is also supported by the large, flat green regions around the pyridine ring on the corresponding curvedness surface. Colour patches on the Hirshfeld surface depend on their closeness to the adjacent molecules and provide information regarding the nearest coordination environment of a molecule. The atoms within 3.8 Å from the HS of ADCP with their respective molecules, involving non-covalent interactions at various levels are displayed in different colour codes in Fig. 4.

The total intermolecular interactions between the promolecule and the exterior molecules were quantified by two-dimensional fingerprint plots (Spackman & McKinnon, 2002) in terms d_i and d_e and are represented as blue regions with dots of varied intensities in Fig. 5. In the fingerprint plots, among all the non-covalent interactions, Cl···H/H···Cl (40.1%) followed by H···H (15.7%) contacts contribute the maximum in the crystal packing of ADCP. The N···H/H···N

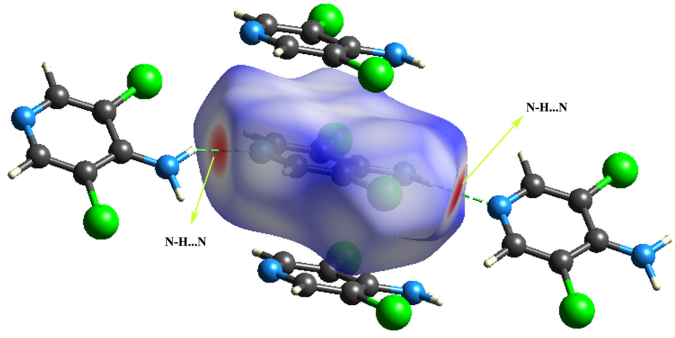

Figure 3
Hirshfeld surface mapped over d_{norm} for ADCP.

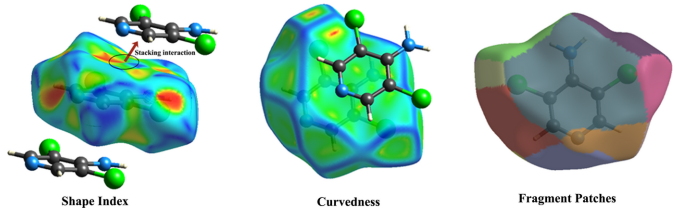

Figure 4
Shape-index, curvedness and colour patches of the molecule within 3.8. Å.

Table 2
The interaction energies (kJ mol^{-1}) of the promolecule with the surrounding molecules within 3.8 Å.

N = number of pairs with that energy; symmetry operation relates that particular colour-coded molecule with the central molecule; *R* is the distance (in Å) between molecular centroids (mean atomic position). B3LYP/6–31G(d,p) electron density was used with scale factors 1.057 (k_{ele}), 0.740 (k_{pol}), 0.871 (k_{dis}) and 0.618 (k_{rep}).

Colour	*N*	Symmetry operation	*R*	E_{ele}	E_{pol}	E_{dis}	E_{rep}	E_{tot}
Red	2	$x+\frac{1}{2}, -y+\frac{1}{2}, z$	8.30	−2.4	−0.1	−4.4	3.9	−4.0
Yellow	2	$-x, -y, z+\frac{1}{2}$	8.88	−1.2	−0.1	−2.9	2.2	−2.5
Fluorogreen	2	$x+\frac{1}{2}, -y+\frac{1}{2}, z$	7.34	−2.2	−0.1	−8.1	5.8	−5.9
Green	2	$-x+\frac{1}{2}, y+\frac{1}{2}, z+\frac{1}{2}$	6.87	−33.8	−8.3	−11.4	37.6	−28.6
Blue	2	$-x+\frac{1}{2}, y+\frac{1}{2}, z+\frac{1}{2}$	6.87	−0.4	−0.4	−5.7	2.1	−4.3
Dark blue	2	x, y, z	3.86	−0.7	−0.8	−33.5	19.6	−18.3
Pink	2	$-x, -y, z+\frac{1}{2}$	6.57	−8.7	−1.5	−10.7	12.9	−11.6

contacts provide a significant contribution (13.1%) through the strong hydrogen bonding involving N and H atoms. The C···H / H···C (7.3%), Cl···Cl (7.1%),C···C (6.8%), N···C/C···N (4.9%) and Cl···C/C···Cl (3.8%) interactions also contribute to the cohesion of the crystal structure.

The stability of the crystal packing arrangement is achieved by the systematic balance between the molecules by which the molecules are aligned to increase the attractive interactions and decrease the repulsive forces to yield the stable and energetically favoured crystalline structure. The total interaction energy (kJ mol^{-1}) is the sum of electrostatic energy, polarization energy, dispersion energy and repulsion energy. The total energy was calculated using the CE-B3LYP/6–31 G(d,p) basis set implemented in *Crystal Explorer 17.5* (Turner *et al.*, 2017) by computing the individual components using the monomer wavefunctions that have been appropriately scaled (k_{ele}= 1.057, k_{pol}= 0.740, k_{dis}= 0.871 and k_{rep}= 0.618) to reproduce the counterpoise-corrected energies B3LYP/6–31 G(d,p) with a small mean absolute deviation of 2.4 kJ mol^{-1} (Mackenzie *et al.*, 2017). The various colour codes in Table 2 indicate the exterior interacting molecules around the distance between molecular centroids (*R*) and the summation of the scaled values of the individual energy components of exterior molecule is given as E_{tot}.

The energy framework analysis reveals the strength of the intermolecular interactions contributing to the crystal packing of the promolecule and its 13 exterior interacting molecules, forming a molecular assembly of 14 molecules. The total and individual energy components of these molecular assemblies were calculated using CE-B3LYP/6–31 G(d,p), resulting in energy frameworks for Coulombic energy, dispersion energy and total energy. These are represented by scaled cylinders with a reference scale of 100. The dimensions of these cylinders reflect the magnitude of the vectorial interaction energy. Fig. 6 shows that electrostatic (Coulombic) interactions make a more significant contribution to the total energy and crystal packing than dispersion interactions among neighbouring molecules.

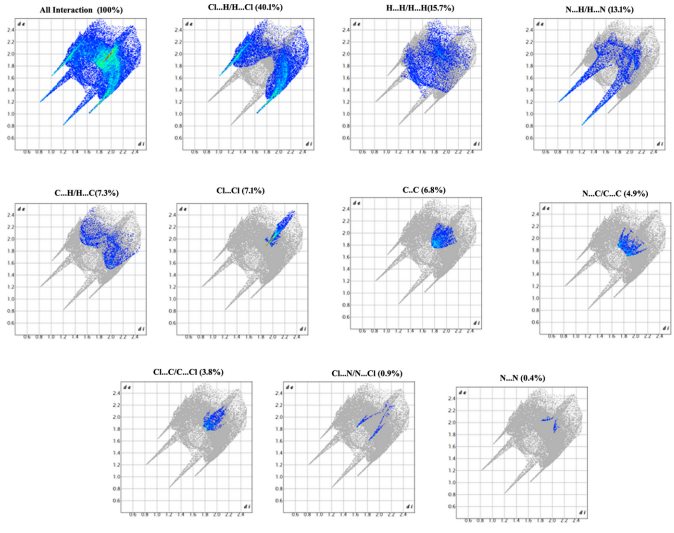

Figure 5
Two-dimensional fingerprint plots of the molecule with percentage contributions.

Synthesis and crystallization

4-Amino-3,5-dichloropyridine (0.04075 mg) was dissolved in 20 ml of water and warmed over a water bath for 20 min at 353 K. The solution was then allowed to cool slowly at room temperature. After a few days, colourless crystals were separated out from the mother liquor.

Refinement

Crystal data, data collection and structure refinement details are summarized in Table 3.

References

Anagnostis, J. & Turnbull, M. M. (1998). *Acta Cryst.* C**54**, 681–683.

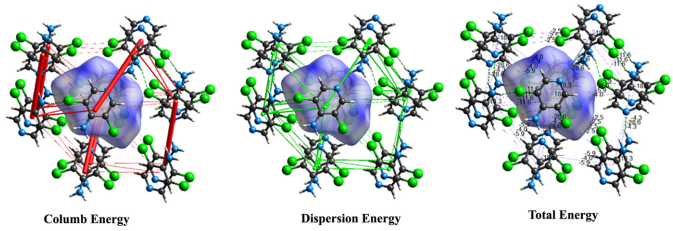

Figure 6
Energy frameworks for ADCP.

Ashokan, A., Nehru, J., Chakkarapani, N., Khamrang, T., Kavitha, S. J., Rajakannan, V. & Hemamalini, M. (2023). *IUCrData*, **8**, x230821.
Boland, S., Alen, J., Bourin, A., Castermans, K., Boumans, N., Panitti, L., Vanormelingen, J., Leysen, D. & Defert, O. (2014). *Bioorg. Med. Chem. Lett.* **24**, 4594–4597.
Bruker (2016). *APEX2* and *SAINT*. Bruker AXS Inc., Madison, Wisconsin, USA.
Cason, C. J. (2004). *POV-RAY* for Windows. Persistence of Vision, Raytracer Pvt. Ltd, Victoria, Australia. http://www.povray.org.
Chung, I. H., Kim, C. S., Seo, J. H. & Chung, B. Y. (1999). *Arch. Pharm. Res.* **22**, 391–397.
Flack, H. D. (1983). *Acta Cryst.* A**39**, 876–881.
Hemamalini, M. & Fun, H.-K. (2010). *Acta Cryst.* E**66**, o1416–o1417.
Hu, Z.-N., Yang, H.-B., Luo, H. & Li, B. (2011). *Acta Cryst.* E**67**, o1138.
Mackenzie, C. F., Spackman, P. R., Jayatilaka, D. & Spackman, M. A. (2017). *IUCrJ*, **4**, 575–587.
Macrae, C. F., Sovago, I., Cottrell, S. J., Galek, P. T. A., McCabe, P., Pidcock, E., Platings, M., Shields, G. P., Stevens, J. S., Towler, M. & Wood, P. A. (2020). *J. Appl. Cryst.* **53**, 226–235.
Malenov, D. P. & Zarić, S. D. (2023). *Chemistry*, **5**, 2513–2541.
McKinnon, J. J., Jayatilaka, D. & Spackman, M. A. (2007). *Chem. Commun.* pp. 3814–3816.
Newell, B. D., McMillen, C. D. & Lee, J. P. (2022). *IUCrData*, **7**, x220804–x220804.
Onnis, V., Cocco, M. T., Fadda, R. & Congiu, C. (2009). *Bioorg. Med. Chem.* **17**, 6158–6165.
Rahman, A. M., Bishop, R., Craig, D. C. & Scudder, M. L. (2003). *CrystEngComm*, **5**, 422–428.
Sheldrick, G. M. (2015*a*). *Acta Cryst.* A**71**, 3–8.
Sheldrick, G. M. (2015*b*). *Acta Cryst.* C**71**, 3–8.
Singaram, K., Marimuthu, D., Baskaran, S. & Chinaga, S. (2016). *J. Chin. Chem. Soc.* **63**, 758–769.
Spackman, M. A. & Jayatilaka, D. (2009). *CrystEngComm*, **11**, 19–32.
Spackman, M. A. & McKinnon, J. J. (2002). *CrystEngComm*, **4**, 378–392.
Spek, A. L. (2020). *Acta Cryst.* E**76**, 1–11.

Table 3
Experimental details.

Crystal data	
Chemical formula	$C_5H_4Cl_2N_2$
M_r	163.00
Crystal system, space group	Orthorhombic, $Pna2_1$
Temperature (K)	296
a, b, c (Å)	13.304 (2), 12.911 (2), 3.8636 (7)
V (Å^3)	663.64 (19)
Z	4
Radiation type	Mo $K\alpha$
μ (mm^{-1})	0.88
Crystal size (mm)	0.33 × 0.23 × 0.22
Data collection	
Diffractometer	Bruker APEXII CCD
No. of measured, independent and observed [$I > 2\sigma(I)$] reflections	5840, 1969, 1729
R_{int}	0.017
$(\sin \theta/\lambda)_{max}$ (Å^{-1})	0.709
Refinement	
$R[F^2 > 2\sigma(F^2)]$, $wR(F^2)$, S	0.031, 0.116, 0.88
No. of reflections	1969
No. of parameters	90
No. of restraints	4
H-atom treatment	H atoms treated by a mixture of independent and constrained refinement
$\Delta\rho_{max}$, $\Delta\rho_{min}$ (e Å^{-3})	0.26, −0.22
Absolute structure	Flack (1983)
Absolute structure parameter	−0.02 (3)

Computer programs: *APEX2* and *SAINT* (Bruker, 2016), *SHELXT* (Sheldrick, 2015*a*), *SHELXL* (Sheldrick, 2015*b*), *PLATON* (Spek, 2020), *Mercury* (Macrae *et al.*, 2020), *POVRay* (Cason, 2004) and *publCIF* (Westrip, 2010).

Turner, M. J., McKinnon, J. J., Wolff, S. K., Grimwood, D. J., Spackman, P. R., Jayatilaka, D. & Spackman, M. A. (2017). *CrystalExplorer17*. The University of Western Australia.
Westrip, S. P. (2010). *J. Appl. Cryst.* **43**, 920–925.

full crystallographic data

IUCrData (2024). **9**, x241120 [https://doi.org/10.1107/S2414314624011209]

4-Amino-3,5-dichloropyridine

Thankappan Ramalakshmi Anantheeswary, Sundaramoorthy Gomathi, Ramu Shyamaladevi, Samson Jegan Jennifer and Ibrahim Abdul Razak

3,5-Dichloropyridin-4-amine

Crystal data

$C_5H_4Cl_2N_2$
M_r = 163.00
Orthorhombic, $Pna2_1$
Hall symbol: P 2c -2n
a = 13.304 (2) Å
b = 12.911 (2) Å
c = 3.8636 (7) Å
V = 663.64 (19) Å^3
Z = 4
$F(000)$ = 328
D_x = 1.631 Mg m^{-3}
Mo $K\alpha$ radiation, λ = 0.71073 Å
Cell parameters from 1969 reflections
θ = 2.2–30.3°
μ = 0.88 mm^{-1}
T = 296 K
Block, colourless
0.33 × 0.23 × 0.22 mm

Data collection

Bruker APEXII CCD diffractometer
φ and ω scans
5840 measured reflections
1969 independent reflections
1729 reflections with $I > 2\sigma(I)$
R_{int} = 0.017
θ_{max} = 30.3°, θ_{min} = 2.2°
h = −17→18
k = −16→18
l = −5→5

Refinement

Refinement on F^2
Least-squares matrix: full
$R[F^2 > 2\sigma(F^2)]$ = 0.031
$wR(F^2)$ = 0.116
S = 0.88
1969 reflections
90 parameters
4 restraints
Hydrogen site location: mixed
H atoms treated by a mixture of independent and constrained refinement
W = 1/[Σ^2(FO^2) + (0.1P)^2] WHERE P = (FO^2 + 2FC^2)/3
$(\Delta/\sigma)_{max}$ = 0.001
$\Delta\rho_{max}$ = 0.26 e Å^{-3}
$\Delta\rho_{min}$ = −0.22 e Å^{-3}
Absolute structure: Flack (1983)
Absolute structure parameter: −0.02 (3)

Special details

Geometry. Bond distances, angles etc. have been calculated using the rounded fractional coordinates. All su's are estimated from the variances of the (full) variance-covariance matrix. The cell esds are taken into account in the estimation of distances, angles and torsion angles

Refinement. Refinement on F^2 for ALL reflections except those flagged by the user for potential systematic errors. Weighted R-factors wR and all goodnesses of fit S are based on F^2, conventional R-factors R are based on F, with F set to zero for negative F^2. The observed criterion of $F^2 > 2\text{sigma}(F^2)$ is used only for calculating -R-factor-obs etc. and is not relevant to the choice of reflections for refinement. R-factors based on F^2 are statistically about twice as large as those based on F, and R-factors based on ALL data will be even larger.

Fractional atomic coordinates and isotropic or equivalent isotropic displacement parameters (Å²)

	x	*y*	*z*	U_{iso}*/U_{eq}
Cl1	0.49802 (4)	0.35972 (5)	0.7165 (4)	0.0500 (2)
Cl2	0.11701 (5)	0.46637 (7)	0.3776 (3)	0.0665 (3)
N1	0.2719 (2)	0.20589 (16)	0.2911 (8)	0.0568 (8)
N2	0.32466 (18)	0.50542 (15)	0.6648 (8)	0.0466 (7)
C1	0.3604 (2)	0.23315 (19)	0.4280 (10)	0.0508 (8)
C2	0.37987 (16)	0.33067 (18)	0.5504 (7)	0.0368 (6)
C3	0.30703 (16)	0.40870 (15)	0.5454 (6)	0.0337 (6)
C4	0.21489 (18)	0.37787 (18)	0.4008 (7)	0.0398 (6)
C5	0.2015 (2)	0.2790 (2)	0.2801 (8)	0.0516 (8)
H1	0.41105	0.18363	0.44048	0.0610*
H1A	0.373 (2)	0.525 (3)	0.788 (12)	0.081 (16)*
H2A	0.2797 (17)	0.5525 (19)	0.653 (10)	0.060 (11)*
H5	0.13951	0.26201	0.18478	0.0620*

Atomic displacement parameters (Å²)

	U^{11}	U^{22}	U^{33}	U^{12}	U^{13}	U^{23}
Cl1	0.0377 (3)	0.0565 (4)	0.0559 (4)	0.0016 (2)	−0.0031 (3)	0.0049 (3)
Cl2	0.0437 (4)	0.0687 (5)	0.0870 (6)	0.0093 (3)	−0.0093 (4)	0.0003 (5)
N1	0.0671 (14)	0.0350 (9)	0.0683 (17)	−0.0125 (10)	0.0056 (14)	−0.0128 (10)
N2	0.0431 (12)	0.0317 (9)	0.0651 (16)	−0.0004 (8)	−0.0017 (11)	−0.0128 (10)
C1	0.0611 (16)	0.0315 (10)	0.0598 (16)	−0.0001 (10)	0.0102 (15)	−0.0035 (11)
C2	0.0369 (11)	0.0323 (9)	0.0412 (11)	−0.0019 (8)	0.0045 (10)	0.0006 (9)
C3	0.0357 (10)	0.0287 (9)	0.0366 (10)	−0.0035 (8)	0.0047 (9)	−0.0012 (8)
C4	0.0372 (11)	0.0420 (10)	0.0401 (12)	−0.0045 (8)	0.0016 (10)	−0.0007 (10)
C5	0.0512 (14)	0.0517 (13)	0.0518 (15)	−0.0208 (12)	0.0009 (12)	−0.0060 (12)

Geometric parameters (Å, º)

Cl1—C2	1.739 (2)	N2—H2A	0.85 (2)
Cl2—C4	1.735 (3)	N2—H1A	0.84 (4)
N1—C1	1.338 (4)	C3—C4	1.405 (3)
N1—C5	1.330 (4)	C4—C5	1.371 (4)
N2—C3	1.352 (3)	C1—H1	0.9300
C1—C2	1.370 (4)	C5—H5	0.9300
C2—C3	1.398 (3)		
C1—N1—C5	116.5 (2)	N2—C3—C4	123.3 (2)
N1—C1—C2	123.0 (2)	Cl2—C4—C3	119.27 (17)
Cl1—C2—C1	119.78 (18)	Cl2—C4—C5	119.9 (2)
Cl1—C2—C3	118.44 (17)	C3—C4—C5	120.8 (2)
C1—C2—C3	121.8 (2)	N1—C5—C4	124.0 (3)
C3—N2—H1A	127 (3)	N1—C1—H1	119.00
C3—N2—H2A	121.2 (18)	C2—C1—H1	118.00
H1A—N2—H2A	111 (3)	N1—C5—H5	118.00

C2—C3—C4	113.97 (19)	C4—C5—H5	118.00
N2—C3—C2	122.7 (2)		
C5—N1—C1—C2	−0.4 (5)	C1—C2—C3—C4	−0.9 (4)
C1—N1—C5—C4	−0.4 (5)	N2—C3—C4—Cl2	−1.1 (4)
N1—C1—C2—Cl1	−178.8 (3)	N2—C3—C4—C5	179.3 (3)
N1—C1—C2—C3	1.1 (5)	C2—C3—C4—Cl2	179.87 (19)
Cl1—C2—C3—N2	−0.1 (4)	C2—C3—C4—C5	0.2 (4)
Cl1—C2—C3—C4	178.94 (19)	Cl2—C4—C5—N1	−179.2 (2)
C1—C2—C3—N2	−180.0 (3)	C3—C4—C5—N1	0.5 (5)

Hydrogen-bond geometry (Å, º)

D—H···*A*	*D*—H	H···*A*	*D*···*A*	*D*—H···*A*
N2—H1*A*···Cl1	0.84 (4)	2.72 (3)	2.983 (2)	100 (3)
N2—H1*A*···Cl1^{i}	0.84 (4)	2.81 (4)	3.625 (3)	164 (3)
N2—H2*A*···Cl2	0.85 (2)	2.66 (3)	3.020 (3)	107 (2)
N2—H2*A*···N1^{ii}	0.85 (2)	2.16 (3)	2.931 (3)	149 (3)

Symmetry codes: (i) −*x*+1, −*y*+1, *z*+1/2; (ii) −*x*+1/2, *y*+1/2, *z*+1/2.